Acta Crystallographica Section A
Foundations of Crystallography
ISSN 0108-7673

Received 19 April 2011
Accepted 15 September 2011

Scattering amplitudes and static atomic correction factors for the composition-sensitive 002 reflection in sphalerite ternary III–V and II–VI semiconductors

M. Schowalter,* K. Müller and A. Rosenauer

Institut für Festkörperphysik, Universität Bremen, D-28359 Bremen, Germany. Correspondence e-mail: schowalter@ifp.uni-bremen.de

Modified atomic scattering amplitudes (MASAs), taking into account the redistribution of charge due to bonds, and the respective correction factors considering the effect of static atomic displacements were computed for the chemically sensitive 002 reflection for ternary III–V and II–VI semiconductors. MASAs were derived from computations within the density functional theory formalism. Binary eight-atom unit cells were strained according to each strain state s (thin, intermediate, thick and fully relaxed electron microscopic specimen) and each concentration ($x = 0, \ldots, 1$ in 0.01 steps), where the lattice parameters for composition x in strain state s were calculated using continuum elasticity theory. The concentration dependence was derived by computing MASAs for each of these binary cells. Correction factors for static atomic displacements were computed from relaxed atom positions by generating $50 \times 50 \times 50$ supercells using the lattice parameter of the eight-atom unit cells. Atoms were randomly distributed according to the required composition. Polynomials were fitted to the composition dependence of the MASAs and the correction factors for the different strain states. Fit parameters are given in the paper.

1. Introduction

The chemical sensitivity of the 002 beam in sphalerite-type semiconductors has been increasingly exploited for quantification of composition in ternary and quaternary semiconductor heterostructures in recent years (Petroff, 1974; Rosenauer *et al.*, 1998; Grillo *et al.*, 2001; Cagnon *et al.*, 2003; Patriarche *et al.*, 2004; Müller *et al.*, 2010). All methods basically measure a quantity depending on the amplitude of the 002 beam from 002 dark-field images or 002 lattice fringe images and normalize it to the value in a region with well known composition (usually the substrate region). Then the composition is determined by a comparison with a series of Bloch-wave simulations.

Cagnon *et al.* (2003) found significant deviations between the measured composition of InGaAs quantum wells and the real composition. The explanation for the deviations was given by Rosenauer *et al.* (2005), who found that structure factors used in the simulations were inaccurate since the simulations were based on structure factors derived from scattering amplitudes computed for isolated atoms (Doyle & Turner, 1968; Weickenmeier & Kohl, 1991) and therefore neglected the redistribution of charge due to bonds. However, the redistribution of charge becomes quite important for structure factors corresponding to small lengths of the scattering vector. Rosenauer *et al.* (2005) introduced the concept of modified atomic scattering amplitudes (MASAs), which enables one to take into account the redistribution of charge easily in Bloch-wave simulations. One has to replace the atomic scattering amplitudes [usually taken from Doyle & Turner (1968) and Weickenmeier & Kohl (1991)] with the corresponding MASAs. Furthermore, the MASA concept also allows one to consider the effect of the static atomic displacements (SADs) due to different covalent radii (Glas, 2003) by correction factors, which are simply premultiplied to the respective MASAs (Rosenauer *et al.*, 2005).

In this paper we computed MASAs and SAD correction factors for the chemically sensitive 002 reflection as a function of composition for different strain states of the ternary sphalerite semiconductor systems $Al_xGa_{1-x}As$/GaAs, GaN_xAs_{1-x}/GaAs, $GaSb_xAs_{1-x}$/GaAs, $GaAs_xSb_{1-x}$/GaSb, $In_xGa_{1-x}P$/GaP, $Ga_xIn_{1-x}P$/InP, ZnS_xTe_{1-x}/ZnTe, $Cd_xZn_{1-x}Se$/ZnSe, $Mg_xZn_{1-x}Se$/ZnSe, $Mg_xZn_{1-x}Te$/ZnTe, ZnS_xSe_{1-x}/ZnSe and $ZnSe_xTe_{1-x}$/ZnTe. Polynomials of order 4 were fitted to the dependence of the MASAs and the correction factors on composition for the different strain states. Fit parameters are given in the paper.

In §2 we briefly review the concept of MASAs (§2.1), give some details on the computation (§2.2) and then list fit parameters in §2.3. §3, which focuses on correction factors for the

static atomic displacements, is subdivided in a similar way: first the concept of the SAD correction factors is introduced (§3.1), then some computational details are listed (§3.2) and, finally, fit parameters are given in §3.3. The concept of the MASAs will be reviewed only briefly because a detailed explanation is given in Rosenauer *et al.* (2005); however, the concept of the SAD correction factors will be introduced in detail, because the concept as presented in Rosenauer *et al.* (2005) was only valid for ternary semiconductors with a varying metal component. The present paper also deals with ternary semiconductors with a varying non-metal component, requiring a generalization of the SAD correction factor concept.

2. Modified atomic scattering amplitudes

2.1. Theoretical background

Simulations in the field of transmission electron microscopy (TEM) require knowledge of the Coulomb potential of the crystalline region used for the simulation. The Coulomb potential is given by its Fourier components, which are proportional to the structure factor $F_\kappa^{hkl}(\mathbf{a})$, with *hkl* indicating the reciprocal-lattice vector, κ the compound and $\mathbf{a}$ representing the three lattice parameters along [100], [010] and [001], which are different in a strained layer.

The structure factor can be written as

$$F_\kappa^{hkl}(\mathbf{a}) = \sum_{j=1}^{8} D_j^{hkl}(T) f_j^{hkl}(\mathbf{a}) \exp[2\pi i \mathbf{g}^{hkl}(\mathbf{a})\mathbf{r}_j], \qquad (1)$$

where the sum index j runs over all the atoms in the unit cell (*i.e.* from 1 to 4 for the metal atoms and from 5 to 8 for the non-metal atoms), $f_j^{hkl}(\mathbf{a})$ is the atomic scattering amplitude (ASA) of atom j with position $\mathbf{r}_j$ and $\mathbf{g}^{hkl}$ is the respective reciprocal-lattice vector depending on the extension of the unit cell. $D_j^{hkl}(T) = \exp[-2\pi^2 i \langle u_j^2(T)\rangle |\mathbf{g}^{hkl}(\mathbf{a})^2|]$ is the Debye–Waller factor at temperature T and $\langle u_j^2(T)\rangle$ is the mean square displacement of atom j. Without loss of generality we will assume the Debye–Waller factor to be 1 in further equations. Usually, ASAs are taken from publications such as Doyle & Turner (1968) or Weickenmeier & Kohl (1991) *etc.*, who parameterized the dependence of computed scattering amplitudes for single atoms as a function of the length of the scattering vector.

The advantage of such a concept is that it is rather general as all compounds can be simulated using scattering amplitudes tabulated for all atoms of the Periodic Table. This is a good approximation for a large number of simulations in TEM and therefore widely used.

However, this concept assumes rotational symmetric scattering amplitudes and therefore neglects the bonds to neighbouring atoms in a specific compound. Within the MASA concept the structure factor may be rewritten as

$$F_\kappa^{hkl}(\mathbf{a}) = \sum_{j=1}^{8} f'^{hkl}_{j,\kappa}(\mathbf{a}) \exp[2\pi i \mathbf{g}^{hkl}(\mathbf{a})\mathbf{r}_j], \qquad (2)$$

where now the ASA $f_j^{hkl}(\mathbf{a})$ has been replaced by the MASA $f'^{hkl}_{j,\kappa}(\mathbf{a})$. Note that, in contrast to the ASA, the MASA has an index κ indicating that the scattering amplitude depends on the compound. For example, the ASA of Ga would be the same in GaN and GaAs, whereas the MASA of Ga in GaN is different from the MASA in GaAs. The advantage of the MASA concept is that it allows the separate treatment of static atomic displacements and Debye–Waller factors for each atom type.

Usually, simulations for a ternary material are carried out within the virtual crystal approximation (VCA). In the VCA the structure factor is linearly interpolated such as

$$F^{hkl}_{A_xB_{1-x}C} = xF^{hkl}_{AC} + (1-x)F^{hkl}_{BC}, \qquad (3)$$

e.g. for a ternary alloy of type $A_xB_{1-x}C$ (analogously for AB_xC_{1-x}).

The VCA in principle describes exactly the structure factor of a ternary alloy when using the isolated-atom approximation. This is easy to see when considering that the sum over all atoms in the unit cell in equation (1) now runs over all atoms in the crystal. One can sort out a portion x of the summands that contribute to F_{AC}^{hkl} and a portion $1-x$ contributing to F_{BC}^{hkl}.

In the MASA concept the VCA is not exact any more, since the MASA of an atom depends on the neighbour of the atom. For example, in GaN_xAs_{1-x} the sum in equation (2) can be re-sorted for all sites with N or As atoms (the neighbour of an N or As atom is always a Ga atom), but cannot be clearly re-sorted for the summands running over the Ga atoms (a Ga atom could have 0, 1, 2, 3 or 4 N neighbours). For each atomic configuration the MASA, in principle, is different. In practice, the respective MASA is then formed by a linear combination. For a random alloy it has been shown already in Rosenauer *et al.* (2005) that this is of lower order.

2.2. Computational details

MASAs are computed using the *Wien2k* software package (Blaha *et al.*, 2001). For a given cell geometry we compute the charge distribution inside the cell self-consistently and then use the 'lapw3' routine within the *Wien2k* package to convert the charge distribution in the unit cell to X-ray scattering amplitudes. Finally these are converted to MASAs.

The cell geometries were selected in the following way. In general the lattice parameters of the two binary semiconductors are different. Therefore, during epitaxy the unit cell will be tetragonally distorted and the lattice parameter in growth direction a_3 will be different from the lattice parameter a_1 and a_2 ($a_1 = a_2 \neq a_3$). Such a situation would correspond to the thick specimen limit (stress parameter $s = 1$, full stress in the electron-beam direction). Another extreme case corresponds to the assumption of an infinitely thin specimen, *i.e.* uniaxial stress ($a_1 \neq a_2 = a_3$, $s = 0$). We also considered an intermediate stress ($s = 0.5$, $a_1 \neq a_2 \neq a_3$) and the bulk material case ($a_1 = a_2 = a_3$). Note that we defined the stress vector as $\sigma_{100} = \sigma$, $\sigma_{010} = s\sigma$ and $\sigma_{001} = 0$. Alternatively it may be expressed as Hooke's law neglecting shear stress:

$$\begin{pmatrix} \sigma_{100} \\ \sigma_{100}s \\ 0 \end{pmatrix} = \begin{pmatrix} c_{11}c_{12}c_{12} \\ c_{12}c_{11}c_{12} \\ c_{12}c_{12}c_{11} \end{pmatrix} \begin{pmatrix} \varepsilon_{100} \\ \varepsilon_{010} \\ \varepsilon_{001} \end{pmatrix}. \quad (4)$$

For each of the four strain states we computed the lattice parameters for concentrations of 0 to 1 in steps of 0.01 by

$$a_i(x, s) = a_{\rm bulk}(x)[1 + \varepsilon_i(x, s)], \quad (5)$$

where $a_{\rm bulk}$ is the bulk lattice parameter and $\varepsilon_i(x, s)$ are the dilatational strains, which are given for a [010] zone axis orientation by

$$\begin{aligned} \varepsilon_{[100]}(x, s) &= f(x), \\ \varepsilon_{[010]}(x, s) &= f(x)\frac{s[c_{11}(x) + c_{12}(x)] - c_{12}(x)}{c_{11}(x) + c_{12}(x)(1 - s)}, \\ \varepsilon_{[001]}(x, s) &= -f(x)\frac{(1 + s)c_{12}(x)}{c_{11}(x) + c_{12}(x)(1 - s)}, \end{aligned} \quad (6)$$

with $c_{ij}(x)$ the elastic constants and $f(x)$ the misfit

$$f(x) = \frac{a_{\rm bulk}(0) - a_{\rm bulk}(x)}{a_{\rm bulk}(x)}, \quad (7)$$

with substrate lattice parameter $a_{\rm bulk}(0)$. The dependence of the lattice parameters on concentration x for the different stress parameters s is shown for GaN_xAs_{1-x} in Fig. 1. (Note that composition evaluations using the 002 beam typically are done in an off-axis orientation close to a [010] zone axis. On the one hand, an evaluation in the [110] zone axis is not recommended owing to dynamical diffraction effects which strongly influence the amplitude of the [002] beam. On the other hand, an off-axis orientation is recommended in order to increase the extinction distance of the (002) reflection and to get a lower thickness dependence of the 002 beam.) (We here restrict the calculations to the [010] zone axis orientation, because an evaluation in *e.g.* a [110] zone axis orientation is not recommended for the reason stated above. However, MASAs for unstrained cells and $s = 1.0$ could be used for other orientations as well provided that strain can be neglected or the specimen can be assumed to be thick.) The concentration dependencies of the elastic constants and bulk lattice parameters are approximated linearly between the respective values of the binary compounds. For each strain state s and concentration x unit cells for both binary materials are generated from the respective set of lattice parameters. These cells are then used to compute the charge distribution within each of the cells using the *Wien2k* code (Blaha *et al.*, 2001).

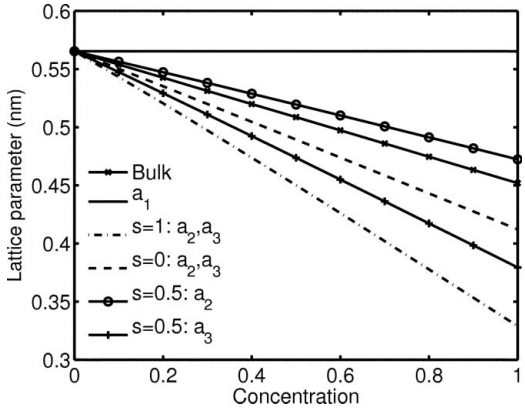

Figure 1
Lattice parameters a_1, a_2 and a_3 for the different stress parameters s as a function of concentration x for GaN_xAs_{1-x}.

In the *Wien2k* package the unit cell is subdivided into spheres with radius $R_{\rm MT}$ around the atom positions (muffin-tin spheres) and the space outside the spheres (interstitial region). In the interstitial region a plane-wave basis set is used, whereas within the muffin-tin spheres the basis set is chosen as an atomic-like basis set with spherical harmonics describing the angular dependence of the wavefunctions. The muffin-tin radii were chosen to be 1% smaller than touching spheres using the 'setrmt' routine. The cutoff for the plane-wave expansion was chosen in such a way that $R_{\rm MT}K_{\rm max} = 7$. The full Brillouin zone was sampled using 5000 k-points for each material. For Mg 3*s*, Zn 3*d* and 4*s*, Cd 4*d* and 5*s*, Al 3*s* and 3*p*, Ga 3*d*, 4*s* and 4*p*, In 4*d*, 5*s* and 5*p*, N 2*s* and 2*p*, P 3*s* and 3*p*, As 3*d*, 4*s* and 4*p*, Sb 4*d*, 5*s* and 5*p*, S 3*s* and 3*p*, Se 3*d*, 4*s* and 4*p* electrons were treated as valence electrons. The convergence with respect to the number of k-points was checked by increasing this number to 10 000 after a first evaluation of the MASAs. As to the exchange and correlation part of the potential, we carried out the computations within both prominent approximations: the local density approximation (LDA) (Ceperley & Alder, 1980) and the generalized gradient approximation (GGA) (Perdew *et al.*, 1996). Results for both approximations are given in §2.3.

Since the unit cell is divided into the different muffin-tin spheres and the interstitial region, the X-ray scattering amplitudes are computed with the 'lapw3' routine separately for each of these regions yielding X-ray scattering amplitudes X_j^{hkl} for each non-equivalent atom j in the unit cell and $X_{\rm inter}^{hkl}$ for the interstitial region. The X-ray scattering amplitudes are then converted to MASAs exploiting the Mott–Bethe formula (Mott, 1930) according to

$$f'^{hkl}_{j,\kappa}(\mathbf{a}) = \frac{e^2 m}{2\pi h_{\rm p}^2 \varepsilon_0 [\mathbf{g}^{hkl}(\mathbf{a})]^2}\left(Z_{j,\kappa} - \frac{X^{hkl}_{j,\kappa}}{\tau_j} - \frac{X^{hkl}_{{\rm inter},\kappa}}{2\tau_j}\right), \quad (8)$$

where m and e are the mass and the modulus of the charge of the electron, respectively, $h_{\rm p}$ is Planck's constant, ε_0 is the electric constant and $Z_{j,\kappa}$ is the nuclear charge of atom j. τ_j is defined as

$$\tau_j = \begin{cases} 4: & 1 \le j \le 4 \\ 4 \times (-1)^{(h+k+l)/2}: & 5 \le j \le 8 \end{cases}, \quad (9)$$

where j from 1 to 4 are metal atoms and from 5 to 8 are non-metal atoms. Equation (8) is non-relativistic and has to be multiplied by the factor

$$1 + (eU/mc^2) \quad (10)$$

for electrons that have been accelerated by a voltage U (c is the speed of light). For a detailed derivation of the definition of MASAs see Rosenauer *et al.* (2005).

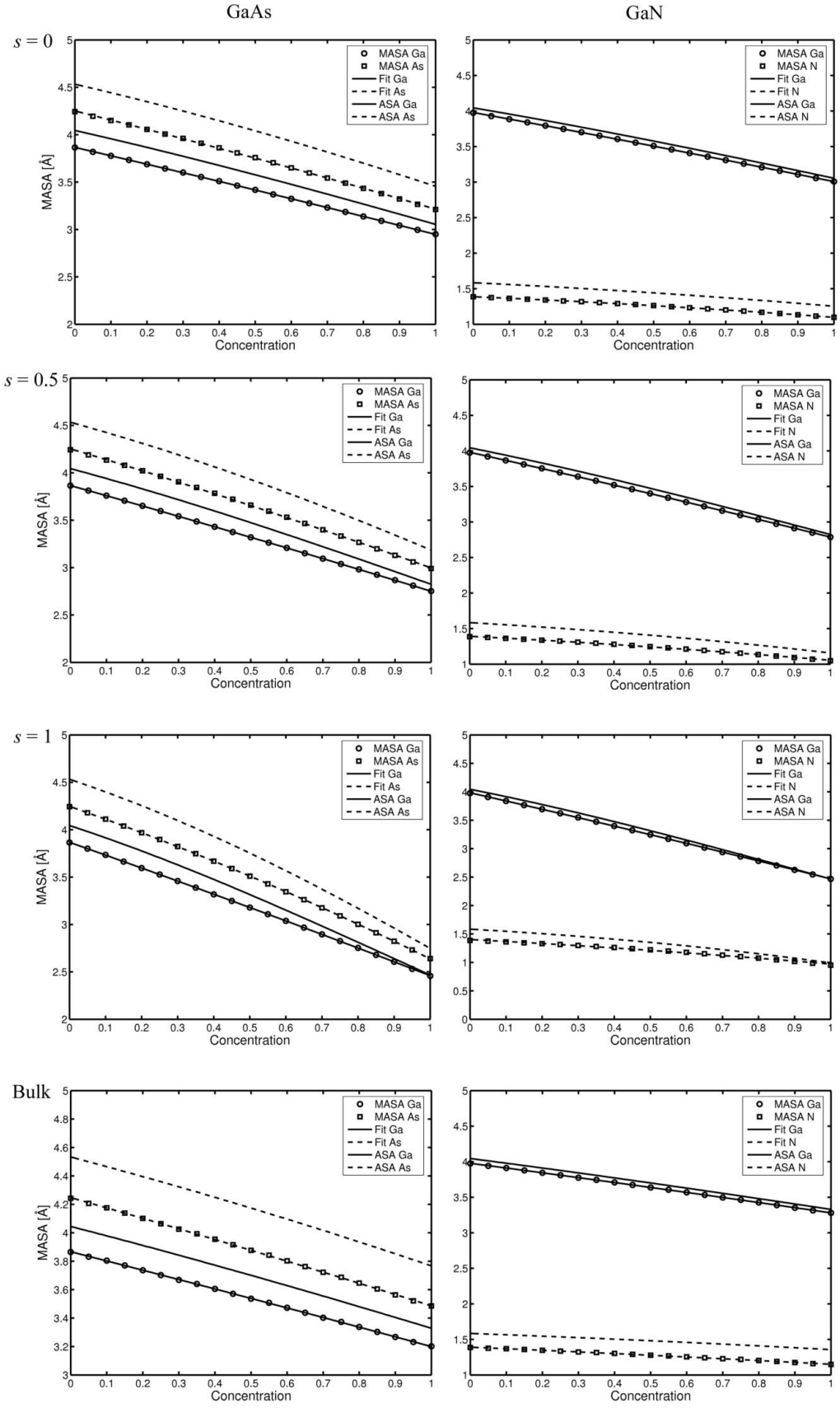

Figure 2
002 MASAs for Ga and As in GaAs, as well as MASAs for Ga and N in GaN are compared with the respective ASAs in the four different strain states considered in this paper. MASAs are plotted as function of N concentration.

Table 1
Polynomial coefficients for the 002 modified atomic scattering amplitudes of strained GaN_xAs_{1-x}/GaAs for different strain states s computed within the LDA using 5000 k-points.

All parameters are given in Å.

		$s = 0.0$	$s = 0.5$	$s = 1.0$	Bulk
GaAs					
Ga	p_1	1.03842E-3	1.02588E-3	1.06949E-3	1.04769E-3
	p_2	−3.86248E-2	−4.59965E-2	−6.35115E-2	−2.20804E-2
	p_3	−8.80587E-1	−1.06997E+0	−1.34430E+0	−6.46214E-1
	p_4	3.86596E+0	3.86592E+0	3.86690E+0	3.86670E+0
	σ	1.18159E-3	8.42658E-4	1.19382E-3	9.15397E-4
As	p_1	1.06816E-3	1.04699E-3	2.85095E-4	1.07483E-3
	p_2	−8.16608E-2	−1.20145E-1	−2.73290E-1	−4.15695E-2
	p_3	−9.55385E-1	−1.13767E+0	−1.33618E+0	−7.20527E-1
	p_4	4.25073E+0	4.25299E+0	4.24644E+0	4.24734E+0
	σ	2.51771E-3	2.52869E-3	1.06964E-3	1.59468E-3
GaN					
Ga	p_1	1.05424E-3	1.05662E-3	1.06819E-3	1.03949E-3
	p_2	−5.27738E-2	−6.37576E-2	−8.11920E-2	−3.67438E-2
	p_3	−9.20624E-1	−1.13022E+0	−1.43385E+0	−6.61840E-1
	p_4	3.97876E+0	3.98074E+0	3.98263E+0	3.97760E+0
	σ	1.63237E-3	1.55445E-3	2.00603E-3	8.87785E-4
N	p_1	6.59401E-4	1.03776E-3	1.23707E-3	1.09651E-3
	p_2	−8.02212E-2	−7.95578E-2	−1.02854E-1	−2.72472E-2
	p_3	−2.10070E-1	−2.58821E-1	−3.30213E-1	−2.13758E-1
	p_4	1.38685E+0	1.39224E+0	1.40229E+0	1.39074E+0
	σ	1.52871E-3	6.62364E-3	1.92194E-2	4.57462E-3

Table 2
Polynomial coefficients for the 002 modified atomic scattering amplitudes of strained GaN_xAs_{1-x}/GaAs for different strain states s computed within the LDA using 10 000 k-points.

All parameters are given in Å.

		$s = 0.0$	$s = 0.5$	$s = 1.0$	Bulk
GaAs					
Ga	p_1	1.02387E-3	1.02145E-3	1.06838E-3	1.04954E-3
	p_2	−3.97432E-2	−4.62031E-2	−6.37383E-2	−2.19771E-2
	p_3	−8.79266E-1	−1.06933E+0	−1.34409E+0	−6.46107E-1
	p_4	3.86566E+0	3.86595E+0	3.86681E+0	3.86678E+0
	σ	1.21225E-3	8.03359E-4	1.13108E-3	8.85770E-4
As	p_1	1.06667E-3	1.04714E-3	2.80100E-4	1.06759E-3
	p_2	−8.17187E-2	−1.20157E-1	−2.73993E-1	−4.20518E-2
	p_3	−9.55324E-1	−1.13787E+0	−1.33561E+0	−7.20695E-1
	p_4	4.25112E+0	4.25320E+0	4.24637E+0	4.24752E+0
	σ	2.63054E-3	2.59490E-3	1.03679E-3	1.44128E-3
GaN					
Ga	p_1	1.05436E-3	1.08137E-3	1.07218E-3	1.03949E-3
	p_2	−5.27922E-2	−6.23101E-2	−8.08219E-2	−3.67336E-2
	p_3	−9.19949E-1	−1.13080E+0	−1.43472E+0	−6.61850E-1
	p_4	3.97848E+0	3.98049E+0	3.98315E+0	3.97761E+0
	σ	1.56255E-3	1.49296E-3	2.13355E-3	8.91004E-4
N	p_1	6.71383E-4	1.03290E-3	1.20109E-3	1.09070E-3
	p_2	−8.00925E-2	−8.05290E-2	−2.07182E-1	−2.74286E-2
	p_3	−2.10003E-1	−2.56694E-1	−2.24140E-1	−2.13923E-1
	p_4	1.38678E+0	1.39174E+0	1.38458E+0	1.39071E+0
	σ	1.57573E-3	7.21451E-3	2.44570E-3	4.24737E-3

Table 3
Polynomial coefficients for the 002 modified atomic scattering amplitudes of strained GaN_xAs_{1-x}/GaAs for different strain states s computed within the GGA using 5000 k-points.

All parameters are given in Å.

		$s = 0.0$	$s = 0.5$	$s = 1.0$	Bulk
GaAs					
Ga	p_1	1.07197E-3	1.03681E-3	1.05925E-3	1.06610E-3
	p_2	−3.46482E-2	−4.14069E-2	−5.99361E-2	−2.02353E-2
	p_3	−8.89160E-1	−1.08021E+0	−1.35510E+0	−6.51472E-1
	p_4	3.86859E+0	3.86873E+0	3.86951E+0	3.86929E+0
	σ	1.25109E-3	8.46729E-4	8.52038E-4	8.79693E-4
As	p_1	1.07064E-3	1.05556E-3	6.81591E-4	1.07216E-3
	p_2	−8.24256E-2	−1.17619E-1	−2.79523E-1	−4.23672E-2
	p_3	−9.57021E-1	−1.14442E+0	−1.33381E+0	−7.21035E-1
	p_4	4.25340E+0	4.25677E+0	4.24855E+0	4.24926E+0
	σ	2.65003E-3	2.89150E-3	1.05823E-3	1.52844E-3
GaN					
Ga	p_1	1.05385E-3	1.01705E-3	1.06391E-3	1.05065E-3
	p_2	−5.20069E-2	−6.96674E-2	−8.03517E-2	−3.58416E-2
	p_3	−9.24960E-1	−1.12818E+0	−1.44004E+0	−6.66043E-1
	p_4	3.98023E+0	3.98086E+0	3.98408E+0	3.97966E+0
	σ	1.53382E-3	1.15768E-3	1.88878E-3	9.66786E-4
N	p_1	7.79309E-4	7.85448E-4	1.25996E-3	1.03039E-3
	p_2	−8.00901E-2	−1.19576E-1	−2.11641E-1	−2.66946E-2
	p_3	−1.99793E-1	−2.06320E-1	−2.04915E-1	−2.06919E-1
	p_4	1.37165E+0	1.37087E+0	1.36925E+0	1.37578E+0
	σ	1.64504E-3	1.28470E-3	2.56099E-3	4.53519E-3

Table 4
Polynomial coefficients for the 002 modified atomic scattering amplitudes of strained GaN_xAs_{1-x}/GaAs for different strain states s computed within the GGA using 10 000 k-points.

All parameters are given in Å.

		$s = 0.0$	$s = 0.5$	$s = 1.0$	Bulk
GaAs					
Ga	p_1	1.07270E-3	1.03933E-3	1.05669E-3	1.06610E-3
	p_2	−3.47364E-2	−4.14547E-2	−6.00611E-2	−2.02353E-2
	p_3	−8.89151E-1	−1.08062E+0	−1.35485E+0	−6.51472E-1
	p_4	3.86867E+0	3.86903E+0	3.86928E+0	3.86929E+0
	σ	1.23812E-3	8.05943E-4	9.13306E-4	8.79693E-4
As	p_1	1.07600E-3	1.05556E-3	7.25804E-4	1.07216E-3
	p_2	−8.17826E-2	−1.17588E-1	−2.79525E-1	−4.23672E-2
	p_3	−9.57359E-1	−1.14441E+0	−1.33390E+0	−7.21035E-1
	p_4	4.25310E+0	4.25667E+0	4.24850E+0	4.24926E+0
	σ	2.60315E-3	2.91055E-3	1.06801E-3	1.52844E-3
GaN					
Ga	p_1	1.05374E-3	1.01693E-3	1.06370E-3	1.05065E-3
	p_2	−5.19830E-2	−6.96003E-2	−8.03855E-2	−3.58416E-2
	p_3	−9.25032E-1	−1.12838E+0	−1.44011E+0	−6.66043E-1
	p_4	3.98023E+0	3.98115E+0	3.98413E+0	3.97966E+0
	σ	1.53247E-3	1.23048E-3	1.92012E-3	9.66786E-4
N	p_1	1.04277E-3	8.45330E-4	1.25238E-3	1.03039E-3
	p_2	−8.08957E-2	−1.20145E-1	−9.01140E-2	−2.66946E-2
	p_3	−1.99292E-1	−2.05926E-1	−3.28838E-1	−2.06919E-1
	p_4	1.37169E+0	1.37086E+0	1.39104E+0	1.37578E+0
	σ	1.61020E-3	1.33710E-3	2.29570E-2	4.53519E-3

2.3. Results

In this part we start by presenting our results for GaN_xAs_{1-x}/GaAs. For the other materials only respective fit parameters are tabulated. Note that we restrict the discussion to 002 MASAs in this paper, because we provide data for composition analysis, which is typically performed in an off-axis condition close to an [010] zone axis. In such a condition the amplitude of the (002) beam is hardly influenced by other structure factors [*e.g.* Bloch-wave simulations for GaAs with a specimen thickness of 30 nm and a centre of Laue circle of (0 20 1.5) result in a (002) beam amplitude of −0.0779 +

$i0.0914$ for Weickenmeier & Kohl ASAs, $-0.0603 + i0.0702$ only 002 ASA substituted by MASA and $-0.0606 + i0.0704$ for all ASAs substituted by MASAs].

In Fig. 2 we show the dependence of the 002 MASAs for Ga and As in GaAs (left column) as well as for Ga and N (right column) on the N concentration x for different strain states s. Note that the calculations were not performed for mixed ternary materials, but for binary cells having lattice parameters **a** computed from the given concentration and strain state (see §2.2). The MASAs were computed using the LDA and 5000 k-points in the full Brillouin zone. To visualize the influence of the redistribution of charge due to bonds on the scattering amplitudes, we also show ASAs taken from Weickenmeier & Kohl (1991) applying the same cell geometries as for the MASA computation.

Because of the tensile strain the MASA decreases with increasing concentration (Titantah *et al.*, 2007). The decrease in the MASA is strongest for the 'thick sample limit' ($s = 1$), because the smallest lattice parameter is in the growth direction.

The dependence of the MASAs on the concentration for each strain state was fitted with fourth-order polynomials according to

$$f'^{hkl}_{j,\kappa}(\mathbf{a}) = p_1(s)x^3 + p_2(s)x^2 + p_3(s)x + p_4(s). \qquad (11)$$

The parameters $p_i(s)$ found for the computations shown in Fig. 2 are given in Table 1. Note that MASAs have to be multiplied with the relativistic factor in equation (10) for relativistic electrons. We also give the maximum deviation σ between the MASAs and the corresponding fit curve. The maximum deviation is smaller than 0.3%, which should be sufficiently precise when comparing with the deviation between the MASAs and the ASAs.

Table 2 gives the corresponding parameter $p_i(s)$ for a similar computation, but 10 000 k-points were used in the full Brillouin zone. Concerning the convergence with respect to the number of k-points one can compare the $p_4(s)$ parameters. The comparison shows that deviations of $p_4(s)$ are significantly smaller than the deviation σ of the fit from the MASA, indicating the convergence with respect to the k-point mesh. Since such deviations were similar for all other material systems, we will only list the fit parameter for 10 000 k-points for these systems.

The influence of the exchange and correlation part of the potential was investigated as well. Tables 3 and 4 give the results as discussed previously for computation carried out using the GGA. Also here the difference between the GGA and the LDA is very small and thus we restrict our list to the LDA results.

Parameters computed using the LDA and 10 000 k-points are given in Tables 5 to 15 in the supplementary material,[1] respectively, for $Al_xGa_{1-x}As/GaAs$, $GaSb_xAs_{1-x}/GaAs$, $In_xGa_{1-x}P/GaP$, $GaAs_xSb_{1-x}/GaSb$, $Ga_xIn_{1-x}P/InP$, $Cd_xZn_{1-x}Se/ZnSe$, $Mg_xZn_{1-x}Se/ZnSe$, $ZnS_xSe_{1-x}/ZnSe$, $Mg_xZn_{1-x}Te/ZnTe$, $ZnS_xTe_{1-x}/ZnTe$ and $ZnSe_xTe_{1-x}/ZnTe$.

[1] Supplementary material for this paper has been deposited in the IUCr electronic archives (Reference: TN5020). Services for accessing these data are described at the back of the journal.

3. Correction factors

3.1. Theoretical background

In a ternary compound the covalent radii of the two atom types sharing the same sublattice are in general different and therefore the lattice will be statically distorted in the vicinity of, for example, an atom A inserted into a binary crystal BC, yielding a ternary compound $A_xB_{1-x}C$. We refer to such distortions as static atomic displacements (SADs). Since the SADs break the translational symmetry of the crystal, the SADs give rise to non-zero structure factors for vectors not belonging to the reciprocal lattice leading to diffuse scattering in between the Bragg spots.

In the presence of SADs the structure factor in the isolated-atom approximation can be written as

$$F^{hkl}(\mathbf{a}) = \frac{1}{N}\sum_{n=1}^{N}\sum_{j=1}^{8} f^{hkl}_{j,n}(\mathbf{a}) \exp\left[2\pi i \mathbf{g}^{hkl}(\mathbf{a})(\mathbf{r}_{j,n} + \mathbf{u}_{j,n})\right], \qquad (12)$$

where now the summation is carried out over N different unit cells of a given crystal with the desired concentration and strain. Note that we do not choose a Debye–Waller factor description of the SADs (see *e.g.* Wang, 1995 or Cowley, 1995), because for such a description the displacements need to be Gaussian distributed (Wang, 1995), a condition that is not fulfilled for all material systems presented in this paper.

The vectors $\mathbf{u}_{j,n}$ are the displacements of atom j in unit cell n being on positions $\mathbf{r}_{j,n}$ in the non-distorted crystal. Since the definition of the SAD correction factors as derived in Rosenauer *et al.* (2005) is limited to ternary materials with a varying group III component, we generalized the derivation of the correction factors. For that we first define the factor $\sigma^k_{j,n}$, which is 1 if the atom of type s is on position j in cell n and zero if not. Second, we define $p^t_{j,n}$, the number of nearest-neighbour atoms of type t to position j in cell n which fulfills $\sum_t p^t_{j,n} = 4$. With these definitions the atomic scattering factor in equation (12) can be substituted as

$$f^{hkl}_{j,n}(\mathbf{a}) \rightarrow \sum_s \sum_t \sigma^s_{j,n} \frac{p^t_{j,n}}{4} f'^{hkl}_{k,\kappa(s,t)}(\mathbf{a}), \qquad (13)$$

where the indices s and t run over all involved elements and $\kappa(s, t)$ specifies the binary compound that can be built out of the elements s and t [*e.g.* s being As and t Ga will result in the same compound $\kappa(s, t)$ = GaAs as s being Ga and t As]. Note also that summands where s and t are from the same elemental group will be zero, because the number of nearest-neighbour atoms being from the same group will be zero. Performing the substitution of equation (13) in equation (12) results in

$$F^{hkl}(\mathbf{a}) = \frac{1}{N}\sum_{n=1}^{N}\sum_{j=1}^{8}\sum_s\sum_t \sigma^s_{j,n}\frac{p^t_{j,n}}{4} f'^{hkl}_{s,\kappa(s,t)}(\mathbf{a}) \times \exp\left[2\pi i \mathbf{g}^{hkl}(\mathbf{a})(\mathbf{r}_{j,n} + \mathbf{u}_{j,n})\right]. \qquad (14)$$

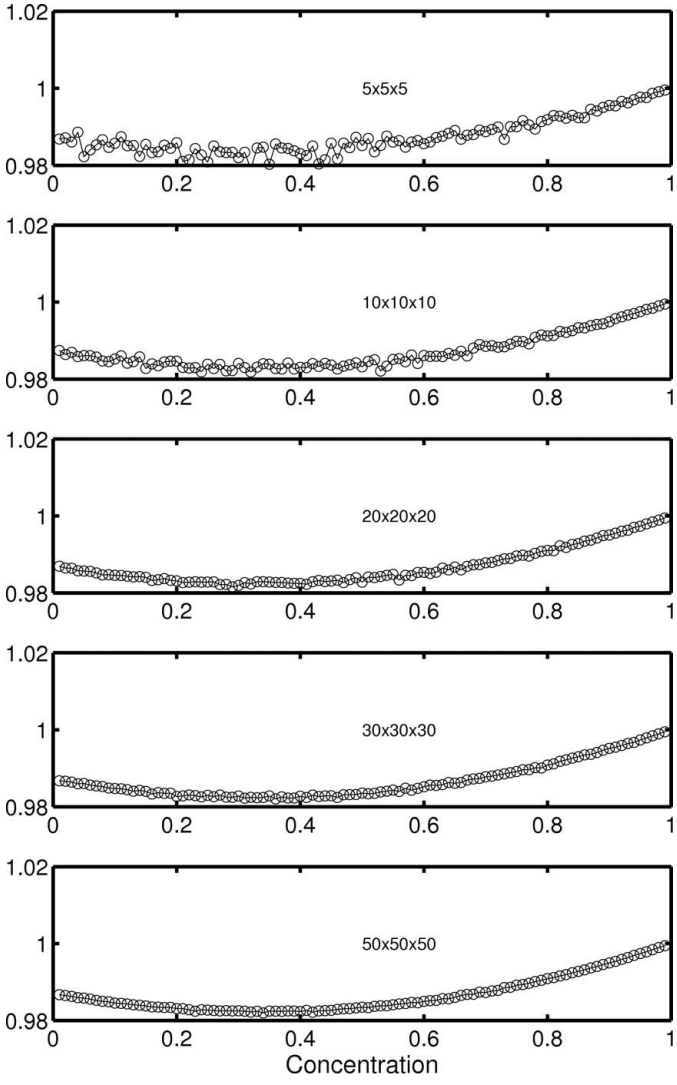

Figure 3
Static atomic correction factor $d^{002}_{\mathrm{Ga,Sb}}$ for different sizes of the supercell as a function of Sb concentration.

Realizing that $\exp[2\pi i\mathbf{g}^{hkl}(\mathbf{a})\mathbf{r}_{j,n}] = \exp[2\pi i\mathbf{g}^{hkl}(\mathbf{a})\mathbf{r}_j] = \tau_j/4$ from equation (9), we can rearrange the summations, yielding

$$F^{hkl}(\mathbf{a}) = \sum_s \sum_t \tau_s x_s x_t d^{hkl}_{s,t} f'^{\,hkl}_{s,\kappa(s,t)}, \qquad (15)$$

with x_s and x_t being the concentrations of element s and t, respectively, and the static atomic correction factor

$$d^{hkl}_{s,t} = \frac{1}{16Nx_s x_t} \sum_{n=1}^{N} \sum_{j=1}^{8} \sigma^s_{j,n} p^t_{j,n} \exp\left[2\pi i\mathbf{g}^{hkl}(\mathbf{a})\mathbf{u}_{j,n}\right]. \qquad (16)$$

Note that this definition can be used for any sphalerite compound, but for the present case of a ternary compound only four of the 16 correction factors are non-zero.

The definition of the static atomic correction factors according to Rosenauer *et al.* (2005) is included in this definition as a special case, in which two different atom types occupy the metal sublattice of the material, whereas only one type of atom is found on the non-metal sublattice.

3.2. Computational details

In order to compute static atomic displacements we first implemented the Keating valence force-field potential (Keating, 1966; Rubel *et al.*, 2008) into the LAMMPS code (Plimpton, 1995). The implementation was tested against the code used in Rubel *et al.* (2008).

Then the lattice parameter sets as a function of the composition (for the four different strain states as described in §2.2) were used and $N \times N \times N$ supercells were generated using these lattice parameter sets. Compositions were generated by randomly distributing the two respective atom types (according to the given concentration) on the respective sublattice. The atom positions within each supercell were relaxed using the programmed Keating potential within the LAMMPS code. We chose an energy convergence criterion of 1×10^{-16} eV, which was very close to the machine's precision.

In order to check convergence of the static atomic correction factors [see equation (16)] with the size of the supercell we computed static atomic correction factors for GaNAs using cells with N = 5, 10, 20, 30, 50. The results are shown in Fig. 3 for $d^{002}_{\mathrm{Ga,Sb}}$. In this graph the cell size of N = 30 leads to results that look quite well converged. However, even with $N = 50$ small fluctuations are still present. A cell size of N = 30 in this graph looks quite well converged. However, small fluctuations are still present with N = 50, that are partly due to the fact that the cell is not yet large enough, but also due to the limited machine precision. Therefore we used N = 50 cells (1 million atom cells) for further computations.

3.3. Results

Computations of the static atomic correction factors for the material systems under consideration within this paper were carried out for the four strain states (s = 0, 0.5, 1.0, bulk) in the concentration range from 0 to 100% in steps of 1%. For the GaNAs/GaAs system, where the large lattice mismatch between cubic GaN and GaAs caused some problems during relaxation for concentrations larger than about 80%, correction factors were computed only up to 80%. Fits were only performed for concentrations up to 80% in this system. In this system realistic concentrations are below about 10% owing to the miscibility gap of GaNAs (Neugebauer & Van de Walle, 1995). Therefore the simulated range covers the experimentally accessible range. The parameters of fourth-order polynomials [equation (11)] were fitted to the concentration dependencies of the computed values.

Fig. 4 shows the computed non-vanishing correction factors in the $GaSb_xAs_{1-x}$/GaAs system for a strain state corresponding to a thick specimen, *i.e.* a tetragonal distorted cell, as a function of Sb concentration x together with their respective polynomials. Small deviations from the polynomial are caused by the finite machine precision of the double variables used within the computer simulations.

The parameters of the polynomials for the different material systems are given in Tables 16 to 27 in the supplementary material.

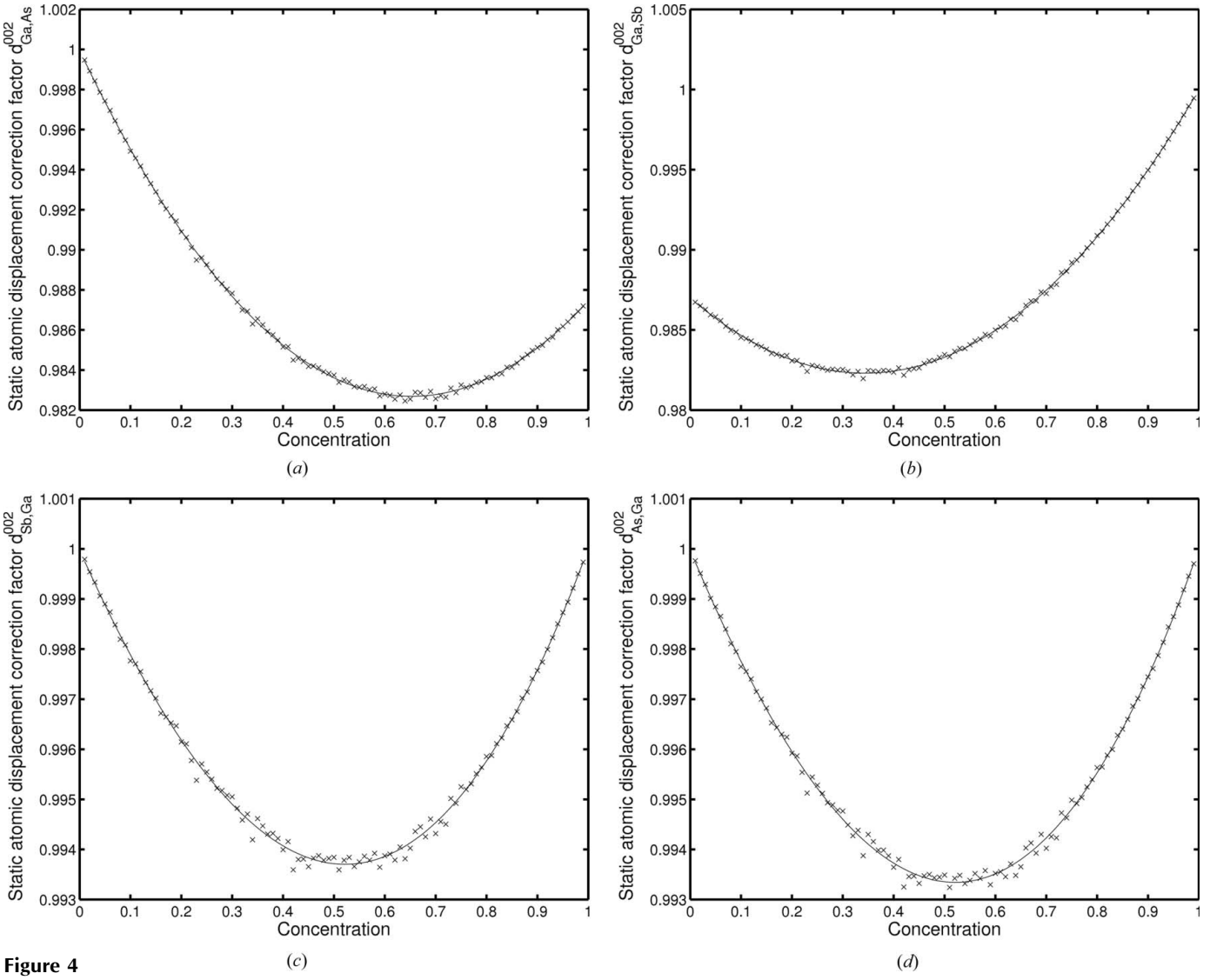

Figure 4
Computed non-vanishing static atomic correction factors for $GaSb_xAs_{1-x}$/GaAs as a function of Sb concentration x with respective fit curves (solid lines) for a strain state corresponding to a thick TEM specimen.

4. Summary

We have computed 002 MASAs for several ternary III–V and II–VI semiconductor systems as a function of the lattice parameter in the [001] direction. The lattice parameter in the [001] direction was adapted according to different strain situations and concentrations. The dependence on concentration was fitted using fourth-order polynomials with parameters given in the paper.

This work was supported by the Deutsche Forschungsgemeinschaft under contract Nos. RO2057/4-1 and SCHO1193/3.

References

Blaha, P., Schwarz, K., Madsen, G. K. H., Kvasnicka, D. & Luitz, J. (2001). *Wien2k, an augmented plane wave + local orbitals program for calculating crystal properties*. Karlheinz Schwarz, Techn. Universität Wien, Austria.

Cagnon, J., Buffat, P. A., Stadelmann, P. A. & Leifer, K. (2003). *Inst. Phys. Conf. Ser.* **180**, 203–206.

Ceperley, D. M. & Alder, B. J. (1980). *Phys. Rev. Lett.* **45**, 566–569.

Cowley, J. M. (1995). *Diffraction Physics*, North-Holland Personal Library, 3rd ed. Amsterdam: Elsevier.

Doyle, P. A. & Turner, P. S. (1968). *Acta Cryst.* A**24**, 390–397.

Glas, F. (2003). *Inst. Phys. Conf. Ser.* **180**, 191–194.

Grillo, V., Albrecht, M., Remmele, T., Strunk, H., Egorov, A. & Riechert, H. (2001). *J. Appl. Phys.* **90**, 3792–3798.

Keating, P. N. (1966). *Phys. Rev.* **145**, 637–645.

Mott, N. F. (1930). *Proc. R. Soc. London Ser. A*, **127**, 658–665.

Müller, K., Schowalter, M., Rubel, O., Volz, K. & Rosenauer, A. (2010). *Phys. Rev. B*, **81**, 075315.

Neugebauer, J. & Van de Walle, C. G. (1995). *Phys. Rev. B*, **51**, 10568–10571.

Patriarche, G., Largeau, L., Harmand, J.-C. & Gollub, D. (2004). *Appl. Phys. Lett.* **84**, 203–205.

Perdew, J. P., Burke, K. & Ernzerhof, M. (1996). *Phys. Rev. Lett.* **77**, 3865–3868.

Petroff, P. M. (1974). *J. Vac. Sci. Technol.* **14**, 973–978.

Plimpton, S. J. (1995). *J. Comput. Phys.* **117**, 1–19.

Rosenauer, A., Fischer, U., Gerthsen, D. & Förster, A. (1998). *Ultramicroscopy*, **72**, 121–133.
Rosenauer, A., Schowalter, M., Glas, F. & Lamoen, D. (2005). *Phys. Rev. B*, **72**, 085326.
Rubel, O., Németh, I., Stolz, W. & Volz, K. (2008). *Phys. Rev. B*, **78**, 075207.
Titantah, J. T., Lamoen, D., Schowalter, M. & Rosenauer, A. (2007). *Phys. Rev. B*, **76**, 073303.
Wang, Z. L. (1995). *Elastic and Inelastic Scattering in Electron Diffraction and Imaging*. New York: Plenum Press.
Weickenmeier, A. & Kohl, H. (1991). *Acta Cryst.* A**47**, 590–597.